Case Studies in Thermal Engineering 22 (2020) 100772

Contents lists available at ScienceDirect

Case Studies in Thermal Engineering

journal homepage: http://www.elsevier.com/locate/csite

Assessment of numerical radiation models on the heat transfer of an aero-engine combustion chamber

Abdelaziz A.A. Gamil *, Theoklis Nikolaidis, Indrit Lelaj [1], Panagiotis Laskaridis

Centre for Propulsion Engineering, Cranfield University, College Rd, Cranfield, Bedford, MK43 0AL, UK

ARTICLE INFO

Keywords:
Gas turbine combustion
CFD
Radiation models
Radiative heat transfer
Discrete ordinates method (DOM)
Spherical harmonics (P-1)

ABSTRACT

Thermal radiation is the most dominant type of heat transfer inside the combustion chamber, which can directly affect the temperature distributions at the combustor walls. This paper provides a comprehensive analysis of the effects of two radiation models on the flame and liner-walls temperatures. A combustion chamber used in the Rolls-Royce-RB-183 turbofan engine was examined in this study by integrating a solid combustor model with the numerical fluid domain. The results indicated that the implementation of radiation models shrinks the flame peak-temperature and altered temperature distribution across the liner. The Discrete Ordinates Method (DOM) estimated a 10% higher temperature at the front part of the liner compared to the non-radiation model and 15% less than the P-1 radiation method. After the dilution zone, the DOM and P-1 models estimated respectively 15% and 25% reduction in the liner temperature compared to the non-radiation combustor. The radiation models have also down predicted the flame temperature by 200 K and more than 200 K for DOM and P-1 case respectively. The results also showed that the emissivity value had minimal effects on the combustor temperature distribution. The DOM considered being more accurate to estimate the combustor wall and flow temperatures compared to the P-1 radiation method.

1. Introduction

The combustion chamber is one of the primary components of gas turbine engines, therefore, the combustor design, performance, and durability are very important parameters which affect the overall gas turbine operation and efficiency [1]. Temperature distribution inside the combustion chamber is an important parameter, which affects the combustor and turbine's durabilities. Thermal radiation is the dominant and the most difficult heat transfer mode to simulate inside the combustion chambers [2]. In some applications, the thermal radiation is responsible for 96% of heat transfer inside the combustion chamber and the combustor walls and hot gases absorb and reflect part of the combustion energy [3,4].

The main types of radiative transfer equation RTE solution are Discrete Ordinates Method (DOM), Spherical Harmonics Method (SHM), and the Photon Monte Carlo (PMC) method [5]. The DOM model is simple to implement, however, it requires a long time to converge for optical thick media [6]. The P-1 method is one of the SHM methods which has been used due to its relative accuracy in some applications and short simulation time [7,8].

In some studies, the DOM and P-1 models have been examined under atmospheric conditions, simple geometries and considering

* Corresponding author.
E-mail address: a.gamil@cranfield.ac.uk (A.A.A. Gamil).
[1] Present address: 110 London Road, Derby, DE12QZ, UK.

https://doi.org/10.1016/j.csite.2020.100772
Received 4 October 2019; Received in revised form 30 June 2020; Accepted 24 October 2020
Available online 2 November 2020

only grey heat radiation [9–11]. However, neglecting the non-grey emission of H2O and CO2 causes insufficient prediction of heat transfer rate inside the combustor [12]. Furthermore, the numerical study of the turbulence radiation interaction for a reactive flow using a single-step mechanism for Methane-Air (G. Li and F. Modest [13]) found that including the heat radiation reduces the flame temperature. The radiative heat loss, using optical thin approximation shrank the peak flame zone [16], which affects the NOx predictions and the increase of/in the net radiative heat fluxes. In addition, optical thin approximation resulted in an overestimation of the heat load to the combustor walls [14]. Additionally, M. Paul and W. Jones [15] have confirmed the suitability of the DOM to solve the radiative heat transfer, however, in their numerical analyses, the heat transfer from fluid-solid-fluid was not explicitly included.

The literature survey showed that limited detailed numerical assessments were found comparing the P-1 and DOM models for aero-engine methane combustion. This paper provides a comprehensive assessment of P-1 and DOM radiation models on combustion liner coupled with conjugate heat transfer by integrating both solid and fluid in the computational domain. In this research, several assessment criteria were combined to intensively evaluate and compare the influences of a radiation model on the flow and wall temperature distributions of a combustor using Methane as burning fuel.

2. Numerical modelling

Turbulent non-premixed methane-air combustion was numerically simulated using ANSYS Fluent through Finite Volume Method (FVM). The transport equations were calculated using second-order discretization methods. Pressure-based solver was employed with SIMPLEC pressure-velocity coupling scheme. A Realizable k-ε (RKE) turbulence model was used in the combustion simulations. The Species Transport used with Eddy Dissipation Model (EDM) model was applied to model the combustion process. The reaction rate of the chemical reactions was inversely proportional to a mixing time τ_t which can be calculated as:

$$\tau_t \equiv \frac{k}{\varepsilon_T} \tag{1}$$

The reaction rate r is obtained from the following equation:

$$r_{EDM} = A\frac{\rho}{\tau_t}\left[\min\left(\min_{i,v'_{ir}\neq 0}\frac{Y_i}{v'_{ir}M_i}, B\frac{\sum Y_i}{\sum v''_{ir}M_i}\right)\right] \tag{2}$$

where A = 4 and B = 0.5 are empirical constants.

One step mechanism was used to describe the combustion of and polynomial coefficients were used to compute specific heat, thermal conductivity and viscosity of the gas as a function of local temperature. The non-premixed one-step reaction mechanism can be expressed as

$$CH_4 + 1.5O_2 \rightarrow CO_2 + 2H_2O \tag{3}$$

DOM and P-1 radiation models were used to assess the radiative heat transfer. Both models were coupled with the weighted sum of the grey-gas model (WSGGM). The overall heat flux was calculated as a summation of each individual grey gas multiplied by the value of its weight in the composition. The absorptivity and emissivity of the hot combustion gases, were calculated as weight-sum of these gases [9,16]. The DOM considers the RTE in the $\vec{s}$ direction as a field equation and the energy equation can be transferred to:

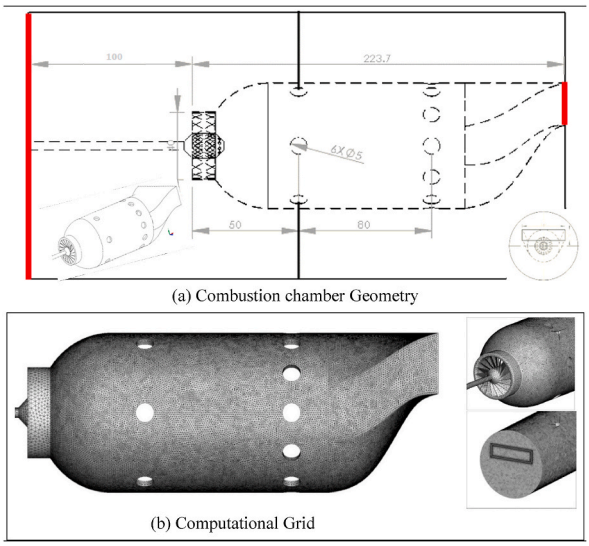

Fig. 1. Combustion chamber geometry and computational grid.

$$\nabla.\left(I_\lambda(\vec{r},\vec{s})\vec{s}+(\alpha_\lambda+\sigma_s)I_\lambda(\vec{r},\vec{s})=a_\lambda n^2 I_{b\lambda}+\left(\frac{\sigma_s}{4\pi}\right)\int_0^{4\pi} I_\lambda(\vec{r},\vec{s}')\Phi(\vec{s}.\vec{s}')\,d\Omega'\right. \tag{4}$$

The transport equation of P-1 radiation model was expressed as:

$$-\nabla.(q_r)=aG-4a\sigma T^4 \tag{5}$$

The radiation flux q_r was calculated using the following equation:

$$q_r=-(1/3(a+s_s)-C\sigma_s)\,\nabla G \tag{6}$$

3. Combustor geometry and computational domain

A tubular gas turbine combustion chamber representing the TAY combustor fitted in a Rolls-Royce RB 183 turbofan engine (Fig. 1) was used in this research. The flame tube consists of a set of six primary holes and twelve dilution holes, The swirler comprises 18 curved vanes oriented at 45° with a thickness of 0.5 mm. The fuel injector has ten 1.7 mm diameter holes located on a cone at 45° with the axis of the combustor.

The CFD model contained both fluid and solid domains. An unstructured tetrahedral grid was generated for the numerical model as shown in Fig. 1. The mesh elements were distributed smoothly over the fluid domain, clustered towards the walls with y+ was between 2 and 22.

Four mesh resolutions between 1.5 million to 11 million were examined. The axial velocity profiles were examined and the numerical results were independent of the mesh number as the grid value exceeds five million. The discrepancy between the 5 million and 11 million models was less than 2%, thus, the mesh with 5 million elements was chosen for the numerical simulations.

4. Boundary conditions

The boundary conditions used in the computational model are shown in Table 1. Mass flow normal to the flow direction was applied at the oxidizer and fuel inlets with turbulence intensities and hydraulic diameters as shown in Table 1. The inlet air was composed of 21% O_2 and 79% N_2 while the fuel was composed of 98.4% CH_4, 0.3% CO_2 and 1.3% N_2. Atmospheric static pressure was applied at the combustor outlet. The material of the liner was assumed as NIMONIC 80-A, and the combustor casing was aluminium (considered as a black body with an emissivity of 1).

5. Validation

Similar to G. Krieger et al. [17], the isothermal velocity profile in the axial location at the area of the primary holes was used as the method of validation in this research. The results of the isothermal flow were validated against the experimental data of A. F. Bicen and W. P. Jones [18] and the numerical results of G. Krieger et al. [17] as shown in Fig. 2. The Numerical results fairly agreed with the experimental data and Krieger et al. [17] with 6% maximum discrepancy in the outlet temperature field.

6. Results and discussion

6.1. Assessment of DOM and P-1 models

Fig. 3 shows the temperature distributions for DOM and non-radiative cases. As demonstrated, the peak flame temperature decreased, and the zone of the highest temperature was shortened when the radiation was taken into account (Fig. 3-A). The temperature reduction was between 100 K and 250 K (13%) (depending on the angle of probe-A in the Y-Z plane), and the combustor liner was subjected to a mean temperature increment of 10 K, roughly 3%. Moreover, the downstream profile (Fig. 4-B) did not follow the same approach as in location (A) with a temperature reduction of 200 K The results of the DOM model agreed well with previous studies such as [1] and [20]. Furthermore, the liner average temperature distribution upstream of the dilution holes is shown in Fig. 3-C. The liner wall temperature increased by approximately 30 K (10%) when wall emissivity was 0.5 and only 10 K (3%) for black body assumption. A similar trend has been demonstrated in the work of R. Dannecker et al. [21]. However, the peak flame temperature

Table 1
Boundary conditions.

	Mass Flow	Temperature	ISA-SLS	Turbulence intensity	Hydraulic diameter [m]
Oxidizer	0.085 kg/s	300 K	In. Ideal gas (0.21 O2 and 0.79 N2)	10%	0.15482
Fuel	0.00163 kg/s	300 K	98% CH4 (mass)	5%	0.0017
Outlet		1000 K		10%	0.04
Casing	Black body (emissivity = 1)				

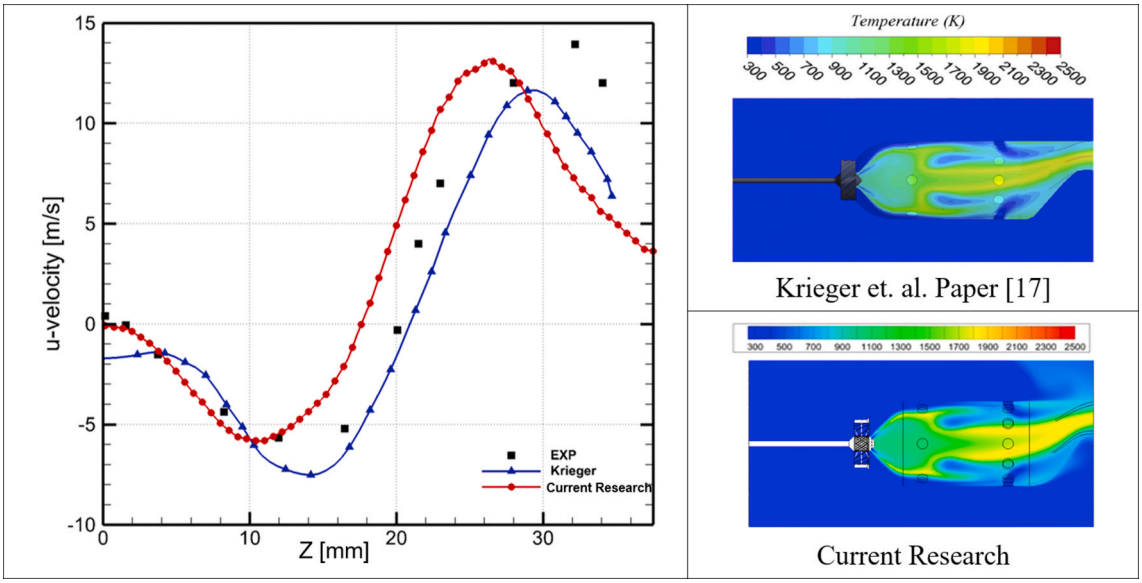

Fig. 2. Validation of numerical solution.

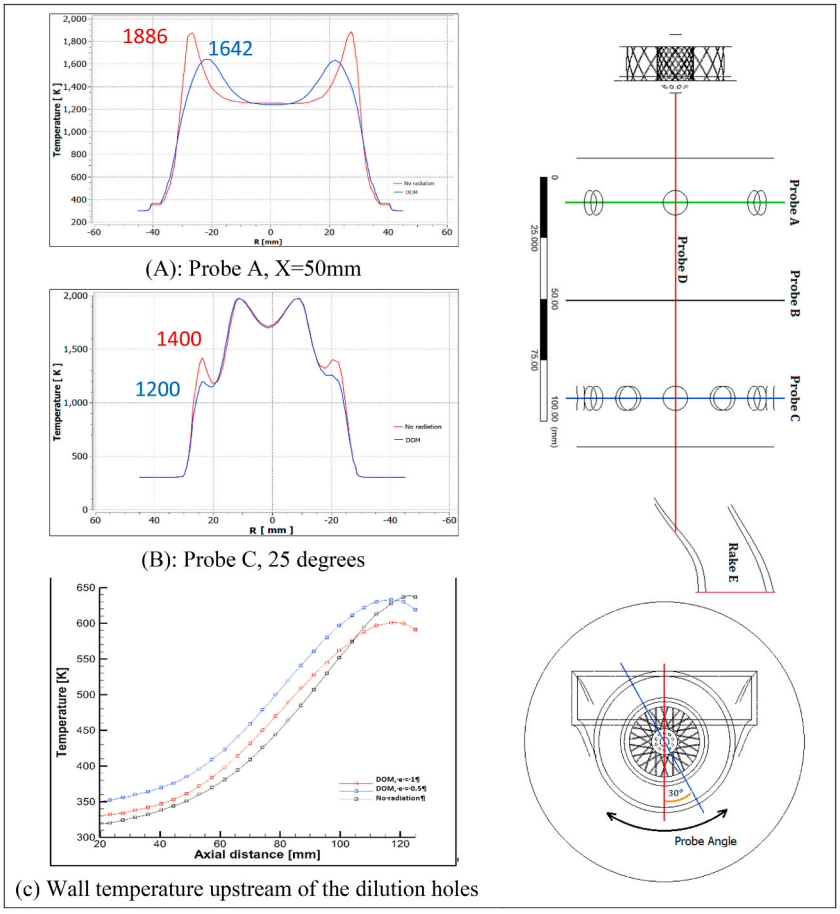

Fig. 3. Temperature distribution for Different Probes.

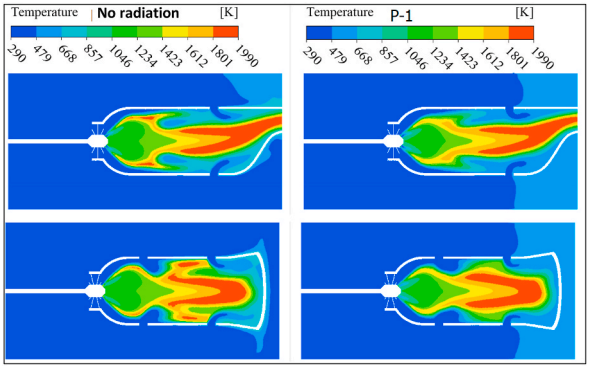

Fig. 4. Temperature Distribution with and without radiation.

was reduced by 15.5% compared to the non-radiation model.

The temperature contours at mid-vertical and mid-horizontal planes (Fig. 4) show that there were minor differences in the temperature profile at the centre of the combustion chamber. However, the utilization of the P-1 model resulted in a temperature reduction near the liner walls at the primary zone and the area downstream to the dilution zone. These findings were in line with G. Li et al. results [13]. Using the P-1 model also resulted in a reduction of more than 200 K in the primary zone average temperature (Fig. 4). This value can go up to 300 K for a grey gas approximation as reported by Modest [12].

6.2. *Comparison of different radiation models*

The comparison between the non-radiation, DOM, and P-1 numerical models (Fig. 5-A) showed that the P-1 radiation predicted a 5% higher liner temperature than DOM and almost 10% higher than the non-radiation case. The effect of radiation models on flame temperature had a similar approach for DOM and P-1 models.

Moreover, by analyzing the wall temperatures (Fig. 5-B), it can be noted that the impact of the radiation model was more obvious in the rear part of the combustion liner. In the front section of the liner, both radiation models increased the mean average temperature of the liner compared to the non-radiation model. However, moving downstream of the dilution holes, radiation models resulted in liner

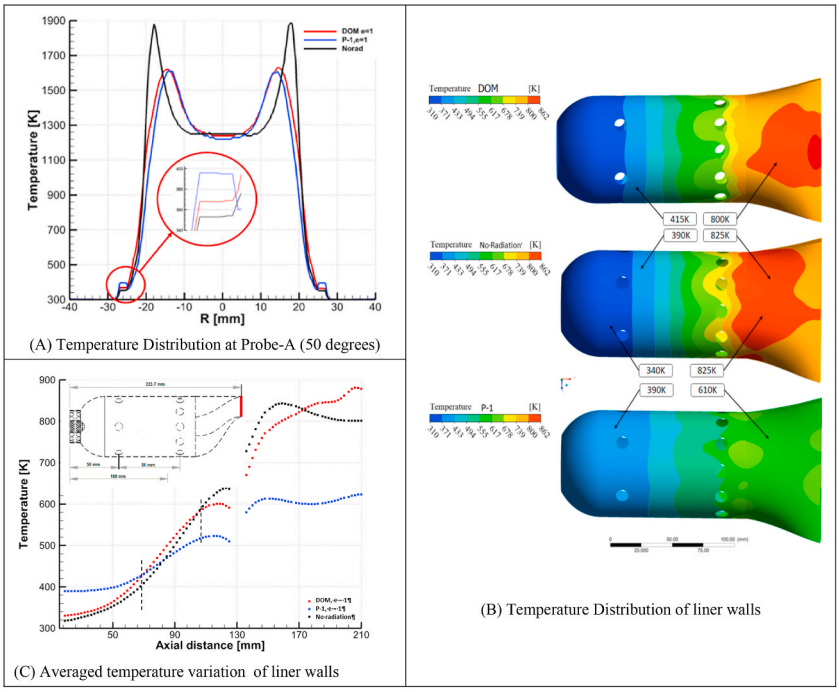

Fig. 5. Comparison of DOM and P-1 radiation models.

Table 2
Combustor exit temperatures using DOM and P-1 model.

CASE	P-1, $\varepsilon = 1$	DOM, $\varepsilon = 0.5$	DOM, $\varepsilon = 1$	No radiation
Max Temp at outlet [K]	1908	1979	1984	1990
Area average Temp at outlet [K]	1031	1047	1048	1052
Max. domain Temp [K]	2054	2057	2054	2230
Pattern Factor	2.25	2.247	2.251	2.22

temperature reductions. This behaviour can also be demonstrated by evaluating the temperature distribution of probe-F, which represents the upper part of the liner wall at the mid-vertical plane (Fig. 5-C). For the DOM model, the front part of the liner (until X = 100 mm) predicted an average increase of the temperature from 5 to 10%, while after X = 100 mm, average liner temperature locally declined by 5% compared to the non-radiation case. It can be also noted that the P-1 model overpredicted the impact of radiation on the liner wall temperature compared to DOM. Locally, P-1 predicted 15% higher wall temperature, for the front part of the chamber (X < 80 mm). Downstream to the dilution holes, there was a small difference between the wall temperature prediction of the DOM and the non-radiation case. The wall temperature of the non-radiation model was higher than the DOM model between the dilution holes up to axial distance X = 170 mm with a maximum discrepancy of 6%. Between the X = 170 mm and the exit of the liner, the DOM model estimated a higher value of wall temperature compared to non-radiation results. This discrepancy increased towards the liner outlet with a maximum value of 10%. The P-1 model predicted 27% lower peak values near the exit at X = 155 mm. In general, the DOM model predicted wall temperature values close to the non-radiation case, while the P-1 estimated a larger discrepancy in temperature values especially near the outlet region of the combustion liner. The largest discrepancy between the radiative models and non-radiation case was located at the front part of the combustor, and the maximum variation (approximately 12%) was between the P-1 and non-radiation model. Similar to previous analysis the DOM model showed closer results to non-radiation simulations, which has been demonstrated in the findings of Mustafa Albas [19]. The small deviation in temperature values at the core of the combustor for different cases showed that the influences of different models was more noticeable at the combustor walls rather than the middle of the liner.

Furthermore, the radiation models reduced the maximum and area averaged temperatures compared to the nonadiabatic case as shown in Table 2. The maximum reduction of maximum outlet and area-averaged temperatures of the P-1 model were 4% and 8% respectively. The DOM models provided a minor maximum temperature variation compared to the nonradiative model. The maximum domain temperature was estimated by approximately 8% for different radiation models. Additionally, the emissivity value did not noticeably affect the temperature profile at the outlet of the combustor.

The above analysis of P-1 and DOM highlighted different aspects of these models and their effects on the temperature distribution inside the combustor. Overall, the findings of this paper agreed well with the previous studies and provided additional detailed comparisons between those models.

7. Conclusions

In this paper, P-1 and DOM radiation models were assessed numerically to highlight their influences on the combustion chamber temperature distribution and the heat transfer process towards the combustor liner. The main findings of this research are:

- The combustor liner was subject to an averaged mean temperature increment of 10 K (3%) using P-1 model compared to non-radiative model.
- DOM model showed 10% increment in the combustor temperature at the front part of the liner compared to the non-radiative case, while P-1 model predicted 15% higher temperature than DOM.
- At the downstream part of the liner, DOM and P-1 models predicted a reduction of 15% and 25% respectively. The peak flame temperature was reduced by 10% (200 K) when DOM was employed, while the reduction of P-1 model was more than 200 K.
- The P-1 radiation model predicted a 5% higher liner temperature than DOM and almost 10% higher than the non-radiation case.
- Changing the liner wall emissivity from 0.5 to 1 did not lead to a noticeable temperature change of the liner nor the outlet profile.
- At the front part of the combustion liner the increased pressure condition resulted in a noticeable increment in liner temperature (20–25%) compared to the atmospheric case, while downstream to the dilution holes this increment was between 10 and 20%.

CRediT authorship contribution statement

Abdelaziz A.A. Gamil: Conceptualization, Methodology, Validation, Supervision, Writing - original draft, Writing - review & editing. **Theoklis Nikolaidis:** Conceptualization, Writing - review & editing, Supervision, Project administration. **Indrit Lelaj:** Methodology, Validation, Investigation, Writing - original draft. **Panagiotis Laskaridis:** Conceptualization, Writing - review & editing, Supervision, Project administration.

Declaration of competing interest

The authors declare that they have no known competing financial interests or personal relationships that could have appeared to

influence the work reported in this paper.

LIST OF NOMENCLATURES

a	Absorption coefficient [1/m]
C	Linear anisotropic phase function
G	Incident radiation [W]
H	Total enthalpy [J]
I_{bn}	Black body intensity or plank function [W/m^2/sr]
I_λ	Wavelength intensity [W/m^2/sr]
k	Turbulence kinetic energy [m^2/s^2]
k_g	Gas thermal conductivity [W/m/K]
k_r	Radiative conductivity [W/m/K]
k_t	Turbulent thermal conductivity
k_w	Wall thermal conductivity [W/m/K]
$l_b/\ s$	Beam length [m]
ln	Spectral radiative intensity obtained from RTE [[w/m^2/sr/Hz]
n	Reflective index
q_{rad}	/ q_r Radiative heat flux [W/m^2]
R	Radial distance from the centreline [mm]
r_{EDM}	Reaction rate
S	Spectral intensity [w/m^2/sr/Hz]
S_h	Fluid enthalpy source term
S_s	Solid enthalpy source term
T	Local temperature [k]

Greek Symbols

ρ	Density [Kg/m^3]
$\alpha_{\varepsilon,\iota}$	Emissivity weighting factor
φ	Equivalence ratio
ε_g	Gas emissivity
ν	Kinematic viscosity [m^2/s]
α_p	Plank mean absorption coefficient or pressure absorption coefficient
σ_s	Scattering coefficient [1/m]
Φ_n	Scattering phase function
Ω	Solid angle [degrees]
α_n	/ α_λ Spectral absorption coefficient
σ	Stephan-Boltzmann constant [W/m^2/K^4]
ε	Total emissivity
λ	Wavelength [m]
τ_t	Mixing time [s]
ε_T	Turbulence dissipation rate [m^2/s^3]

Appendix A. Supplementary data

Supplementary data to this article can be found online at https://doi.org/10.1016/j.csite.2020.100772.

References

[1] W.P. Law, J. Gimbun, Scale-adaptive simulation on the reactive turbulent flow in a partial combustion lance: assessment of thermal insulators, Appl. Therm. Eng. 105 (2016) 887–893.
[2] A.K. Sharma, C. Bhattacharya, S. Sen, A. Mukhopadhyay, A. Datta, "Analysis of Different Radiation Models in a Swirl Stabilized Combustor," ASME 2014 Gas Turbine India Conference, GTINDIA 2014, New Delhi, India, 2014.
[3] Rolls-Royce, 2018. "RB-183" [Online]. Available, https://www.rolls-royce.com/. (Accessed 8 May 2018).
[4] H. Ziebland, R.C. Parkinson, "Heat Transfer in Rocket Engines," AGARDograph No. 148, 1971.
[5] M.F. Modest, F. Michael, Radiative Heat Transfer, Academic Press, 2003.
[6] N. Kayakol, N. Selçuk, I. Campbell, Ö.L. Gülder, Performance of discrete ordinates method in a gas turbine combustor simulator, Exp. Therm. Fluid Sci. 21 (1–3) (2000) 134–141.
[7] L. Wang, D.C. Haworth, S.R. Turns, M.F. Modest, Interactions among soot, thermal radiation, and NOx emissions in oxygen-enriched turbulent nonpremixed flames: a computational fluid dynamics modeling study, Combust. Flame 141 (1–2) (2005) 170–179.

[8] L. Wang, M.F. Modest, D.C. Haworth, S.R. Turns, Modeling nongray gas-phase and soot radiation in luminous turbulent nonpremixed jet flames, Combust. Theor. Model. 9 (4) (2005) 673–691.
[9] M.F. Modest, D.C. Haworth, Radiative Heat Transfer in Turbulent Combustion Systems: Theory and Applications, Springer, 2016.
[10] M.H. Bordbar, G. Wecel, T. Hyppänen, A line by line based weighted sum of gray gases model for inhomogeneous CO2-H2O mixture in oxy-fired combustion, Combust. Flame 161 (9) (2014) 2435–2445.
[11] S. Shan, B. Qian, Z. Zhou, Z. Wang, K. Cen, New pressurized WSGG model and the effect of pressure on the radiation heat transfer of H2O/CO2gas mixtures, Int. J. Heat Mass Tran. 121 (2018) 999–1010.
[12] M.F. Modest, D.C. Haworth, Radiative Heat Transfer in Turbulent Combustion Systems, Springer, 2013, p. 151.
[13] G. Li, M.F. Modest, "Numerical simulation of turbulence–radiation interactions in turbulent reacting flows, Model. Simul. Turbul. Heat Transf. 15 (2005) 69–102.
[14] T. Ren, M.F. Modest, S. Roy, Monte Carlo simulation for radiative transfer in a high-pressure industrial gas turbine combustion chamber, J. Eng. Gas Turbines Power 140 (May) (2017) 1–10.
[15] M.C. Paul, W.P. Jones, Radiative heat transfer in a model gas turbine combustor, WIT Trans. Eng. Sci. 53 (2006) 413–421.
[16] John D. Anderson, Computational Fluid Dynamics the Baiscs with Applications, McGraw-Hill, 1995.
[17] G.C. Krieger, A.P.V. Campos, M.D.B. Takehara, F. Alfaia Da Cunha, C.A. Gurgel Veras, Numerical simulation of oxy-fuel combustion for gas turbine applications, Appl. Therm. Eng. 78 (2015) 471–481.
[18] A.F. Bicen, W.P. Jones, Velocity characteristics of isothermal and combusting flows in a model combustor, Combust. Sci. Technol. 49 (1–2) (1986) 1–15.
[19] M. Ilbas, The effect of thermal radiation and radiation models on hydrogen-hydrocarbon combustion modelling, Int. J. Hydrogen Energy 30 (10) (2005) 1113–1126.
[20] V. Kez, F. Liu, J.L. Consalvi, J. Stroehle, B. Epple, A comprehensive evaluation of different radiation models in a gas turbine combustor under conditions of oxy-fuel combustion with dry recycle, J. Quant. Spectrosc. Radiat. Transf. 172 (2016) 121–133, https://doi.org/10.1016/j.jqsrt.2015.11.002.
[21] R. Dannecker, K.U. Schildmacher, B. Noll, R. Koch, M. Hase, W. Krebs, M. Aigner, Impact of radiation on the wall heat load at a test bench gas turbine combustion chamber: measurements and CFD simulation, in: Proceedings of the ASME Turbo Expo 2007: Power for Land, Sea, and Air, 4, 2007, pp. 1311–1321, https://doi.org/10.1115/GT2007-27148.